FISEVIER

Contents lists available at ScienceDirect

Journal of Membrane Science

journal homepage: www.elsevier.com/locate/memsci



Breaking separation limits in membrane technology

Juan-Manuel Restrepo-Flóreza, Martin Maldovana, b, s

- ^a School of Chemical & Biomolecular Engineering, Georgia Institute of Technology, Atlanta, GA 30332, USA
- ^b School of Physics, Georgia Institute of Technology, Atlanta, GA 30332, USA



ARTICLE INFO

Keywords:
Polymeric membrane
Gas separation
Anisotropic transfer

ABSTRACT

Membrane separation processes are efficient and sustainable alternatives to energy intensive distillation operations. In gas separations, polymeric membranes dominate the landscape of industrial applications and many improvements in performance hinge on the ability to tailor the chemistry of polymeric materials. The basic goal in membrane separations is to control the solubility and diffusivity of the chemical compounds in order to tailor the relative magnitude of the fluxes of the chemical species across the membrane. In this paper, we introduce a fundamentally new separation device that uses an anisotropic polymeric membrane to guide molecular transport to specific spatial locations. Our proposed separation device enables to manipulate the flux direction of compounds, in addition to the flux magnitude, thus adding a new tool to separate chemical species. We report unprecedented selectivities for O_2/N_2 separation – up to two orders of magnitude larger than conventional membranes.

1. Introduction

Membrane separation technologies are critically important for the development of sustainable industrial processes for global chemical production [1-4]. Separations based on membranes are less energy intensive than typical separation operations such as distillation and drying because membranes do not require phase changes [2-5]. Importantly, during the last decades, gas separation based on non-porous membranes have attracted considerable attention due to their low costs and improved efficiencies [5–8]. In non-porous membranes, separations are generally described by a solution-diffusion model involving a twostep mechanism: initial molecule absorption into the membrane followed by diffusive molecular transport under a chemical potential gradient [9]. The membrane efficiency for separating a binary mixture made of compounds A and B is generally measured by the ratio $\alpha_{A/B}$ of the normalized fluxes with respect to the driving forces across the membrane (i.e. selectivity). The basic principle fueling most research on membrane separations is that large selectivities $\alpha_{A/B}$ can be achieved by manipulating the diffusivity and solubility of compounds A and B such that the flux of A is increased while the flux of B is reduced [4-7,10-13]. An established approach to achieve such enhanced membranes is to tailor chemical and structural properties of the membrane material in order to affect the physical mechanisms that govern the diffusivities and solubilities of compounds A and B[4-6,13-16]. In the ideal case, the engineered material would yield a

membrane where the selectivity $\alpha_{A/B}$ and the flux $J_{\rm A}$ of the compound of interest are both maximized. This principle has been successfully used for the design and fabrication of membranes that are at the commercial stage and also under research development [5–8]. Additionally, process engineering using multistage modules or internally staged permeators has been applied to increase the purity of the products [17–19].

Here we propose the development of a new class of separation processes by designing anisotropic membranes that can guide molecular transport to specific locations. We note that established approaches for mass separation assume that the membrane material is isotropic. This means that mass-flow cannot be "guided" in controlled ways to perform separations. In contrast, we propose rationally designed anisotropic membranes that purposely guide molecular diffusion to specific places and this translates into a completely new physical mechanism to improve current separation processes. Contrarily to conventional isotropic membranes, the use of anisotropic membranes allows controlling both *direction* and *magnitude* of the mass flux. Significantly, using our anisotropic design we found remarkable selectivities for O_2/N_2 separations, up to two orders of magnitude higher than those obtained with the best available isotropic polymer.

We show in Fig. 1(b) how our separation device that controls the direction of mass flow using an anisotropic membrane operates significantly different from typical isotropic membranes such as planar, hollow fibers, or dual-layer hollow fiber membranes. In the isotropic case, membranes separate two compounds by selectively permeating

^{*} Corresponding author at: School of Chemical & Biomolecular Engineering, Georgia Institute of Technology, Atlanta, GA, 30332, USA E-mail address: maldovan@gatech.edu (M. Maldovan).

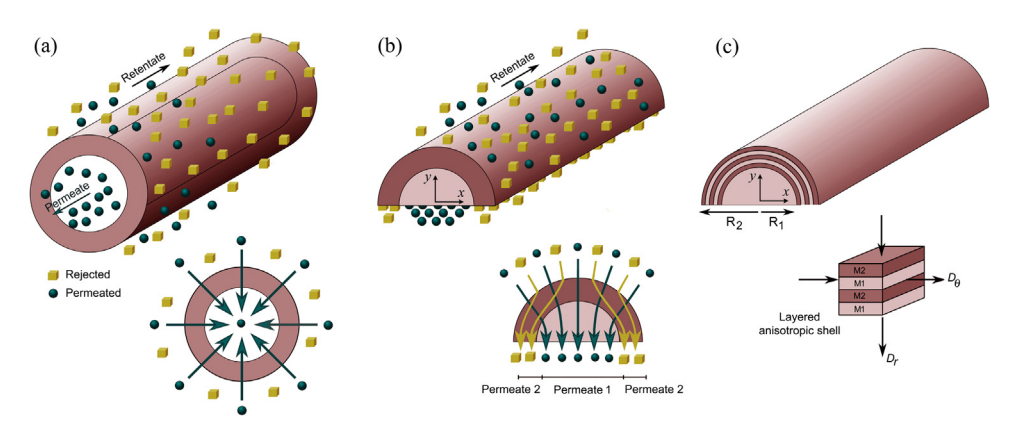


Fig. 1. (a) Isotropic hollow fiber working for separation in countercurrent flow. The cylindrical membrane is highly selective for compound A (spheres) thus creating a permeate enriched in A. Inset shows the radial flux lines due to the cylindrical symmetry. (b) Proposed anisotropic membrane separation device consisting of an isotropic cylindrical core of radius R_1 covered by an anisotropic cylindrical shell with internal radius R_1 and external radius R_2 . In this case, the two molecules (spheres and cubes) permeate in the membrane. The schematics show the ideal case where one compound (cubes) is directed around the core and the other compound (spheres) is focused towards the core. We are interested in collecting

molecules A (spheres) at the core region ($-R_1 < x < R_1$, y = 0). Inset shows the flux lines for the two compounds, which are bent as a consequence of the anisotropicity of the shell. Simultaneous control of the flux trajectory for the two compounds is the basic principle of operation of the anisotropic membrane. (c) The anisotropic shell can be constructed using multilayer structures made of two isotropic materials M_1 and M_2 with mass resistances adding in series in the radial direction and in parallel in the azimuthal direction.

one compound through the membrane while rejecting the other one [Fig. 1(a)]. As a result, two streams with different compositions develop - a permeate enriched with the permeated compound and a retentate enriched with the rejected compound [7,9]. In contrast, the proposed separation device using an anisotropic membrane [Fig. 1(b)] is selective for one of the compounds by simultaneously guiding the molecules that have permeated into the membrane toward different locations on the "permeate" side. Three streams develop: the retentate and two permeate fractions, with compositions that depend on the effectiveness of the anisotropic membrane to reroute the different species. Also note that our separation device does not possess a hollow core but rather a solid material core, in contrast to hollow fiber membranes. Furthermore, separation processes in hollow fiber membranes occur under a one-dimensional radial concentration gradient [Fig. 1(a)], while our device requires a two-dimensional concentration gradient for operation [Fig. 1(b)]. It is important to highlight that control over flux direction as considered in this paper has already been proven both experimentally and theoretically for mass and heat diffusion but has not been used for gas separation [20-25]. A number of fundamental questions arise when considering anisotropic membranes for separation. What structural geometry would allow taking full control of the direction of mass flux and separation capabilities? How does an anisotropic membrane perform in comparison with a typical isotropic membrane? And how can we construct such anisotropic membrane considering that most currently available membrane materials are isotropic? In this paper, we address these questions in the context of gas separations and prove that anisotropic layered structures made of isotropic materials can be used to enhance the separation performance of typical isotropic membranes breaking the limits imposed by the conventional upper bound relation. Specifically, we discuss these findings in the case of O2/N2 separation where we propose a structure/material design consisting of rationally arranged isotropic polymeric materials. Enhancing O2/N2 gas separation is important since highly-efficient O2/N2 separation has been challenging with current membrane materials. The large amount of tabulated data for the diffusion properties of O₂ and N₂ in different polymers facilitates material selection to achieve O2 and N2 anisotropic diffusion and separation. Clearly the proposed concept for separation can also be applied to other gas mixtures.

2. Methods

Diffusive transport processes in isotropic membranes are commonly described by Fick's theory, which establishes that the flux J of species i across a planar membrane and the selectivity α are given by

$$J_{i} = \frac{D_{i}S_{i}\Delta p_{i}}{L}, \quad \alpha_{A/B} = \frac{J_{A}/\Delta p_{A}}{J_{B}/\Delta p_{B}} = \left(\frac{D_{A}}{D_{B}}\right)\left(\frac{S_{A}}{S_{B}}\right) \tag{1}$$

where D_i is the diffusivity, S_i the solubility, Δp_i the driving force, and L the membrane thickness [1,13–16]. In contrast, in our proposed device, anisotropic material properties are engineered to obtain a specific functionality. This can be achieved by engineering the mass diffusivity tensor [21,26–30]

$$J_{(i)} = - \begin{bmatrix} D_{xx(i)} & D_{xy(i)} \\ D_{yx(i)} & D_{yy(i)} \end{bmatrix} \nabla C_{(i)}$$
(2)

In order to design separation processes using engineered anisotropic membranes, the first task is to define a suitable structural geometry. In the case of isotropic membranes, this selection is performed by considering that the system should fit standard module designs and be easy to manufacture and maintain [1,5,8]. In anisotropic membranes, however, it is also necessary to find a structural geometry that allows the easy collection of the permeate fraction of interest. Towards this end, we introduce a membrane separation device consisting of two concentric half-cylinders as shown in Fig. 1(b). The cylindrical core of radius R_1 is made of an isotropic material I with solubility $S_{I(i)}$ and diffusivity $D_{I(i)}$ for compound i. On the other hand, the cylindrical shell with internal radius R_1 and external radius R_2 is made of an anisotropic material with solubility $S_{II(i)}$ and tensorial diffusivity $\overline{D}_{II(i)}$. The role of the anisotropic shell is to manipulate the trajectory of the molecules of interest. For example, an ideal anisotropic shell for separation of a binary mixture should detour one compound around the core and focus the other compound towards the core [26,31]. The effectiveness of the anisotropic shell for separation will thus depend on the ability of the shell to differently promote the diffusion of the compounds along the radial and azimuthal directions. Note that in our proposed design, the permeate fraction enriched with the compound of interest is collected at the planar lower surface of the cylindrical core, i.e. at the line $-R_1 < x < R_1, y = 0.$

Our initial objective is to show how the anisotropic shell affects separation of a binary mixture of arbitrary compounds A and B. The diffusion of species i (A or B) in the core and shell regions can be described using continuity and Fick's law Eqs. (1) and (2), which yields the following differential equations for diffusion

$$\frac{1}{r}\frac{\partial}{\partial r}\left(r\frac{\partial C_{I(i)}}{\partial r}\right) + \frac{1}{r^2}\frac{\partial^2 C_{I(i)}}{\partial \theta^2} = 0 \text{ for the core}$$
(3)

$$\frac{1}{r}\frac{\partial}{\partial r}\left(r\frac{\partial C_{II(i)}}{\partial r}\right) + \frac{l_{(i)}^2}{r^2}\frac{\partial^2 C_{II(i)}}{\partial \theta^2} = 0 \text{ for the shell}$$
(4)

where $l_{(i)}^2 = D_{\theta(i)}/D_{r(i)}$, $D_{\theta(i)}$ and $D_{r(i)}$ are the azimuthal and radial

diffusion coefficients of the shell, respectively. Eqs. (3) and (4) have solutions $C_i(r,\theta)=Y_i(r)G_i(\theta)$ in the form of Fourier's series expansion [32]. By considering the mirror symmetry with respect to x=0 and a non-divergent concentration at r=0, the spatial concentrations $C_i(r,\theta)$ can be written as

$$C_{I(i)}(r,\theta) = C_{I(i)}^{0} + \sum_{n=1}^{\infty} a_{n(i)} r^{n} \sin(n\theta)$$
 (5)

$$C_{II(i)}(r,\theta) = C_{II(i)}^{0} + \sum_{n=1}^{\infty} \left[b_{n(i)} r^{nl(i)} + c_{n(i)} r^{-nl(i)} \right] \sin(n\theta)$$
(6)

where the constants $C_{I(i)}^0$, $C_{II(i)}^0$ and the coefficients $a_{n(i)}$, $b_{n(i)}$ and $c_{n(i)}$ are obtained by applying the following boundary conditions. We consider a partial pressure p_i on the upper side $(r=R_2)$ and zero at the bottom of the device $(\theta=0)$. Note we use only two pressures in contrast to multistage membrane permeators. At the interface between shell and core $(r=R_1)$ we enforce the continuity of the radial flux and the discontinuity in concentration by considering the partition coefficient $K_{(i)}=S_{I(i)}/S_{II(i)}$. We thus have

$$\begin{split} D_{I(i)} \frac{\partial C_{I(i)}}{\partial r} &= D_{r(i)} \frac{\partial C_{II(i)}}{\partial r}, \quad C_{I(i)} = K_i C_{II(i)} \quad \text{at} \quad r = R_1 \\ C_{II(i)} &= p_{(i)} S_{II(i)} & \text{at} \quad r = R_2 \\ C_{I(i)} &= 0; \quad C_{II(i)} = 0 & \text{at} \quad \theta = 0 \end{split} \tag{7}$$

The above boundary conditions yield the following expressions for the concentration of each compound i

$$C_{I}(r,\theta) = \sum_{n=1}^{\infty} \alpha_{n} \left(2 K l D_{r}' \right) \left(\frac{r}{R_{1}} \right)^{n} \sin(n\theta)$$

$$C_{II}(r,\theta) = \sum_{n=1}^{\infty} \alpha_{n} \left[(lD_{r}' + K) \left(\frac{r}{R_{1}} \right)^{nl} + (lD_{r}' - K) \left(\frac{r}{R_{1}} \right)^{-nl} \right] \sin(n\theta)$$

$$\alpha_{n} = PS_{II} \frac{2}{\pi} \left[\frac{1 - (-1)^{n}}{n} \right] \left[(lD_{r}' + K) \left(\frac{R_{2}}{R_{1}} \right)^{nl} + (lD_{r}' - K) \left(\frac{R_{2}}{R_{1}} \right)^{-nl} \right]^{-1}$$
(8)

and $C_{I(i)}^0 = C_{II(i)}^0 = 0$, where $D_{r(i)}' = D_{r(i)}/D_{I(i)}$. We validated the concentrations $C_i(r,\theta)$ given by Eq. (8) against numerical predictions via COMSOL Multiphysics and obtained excellent agreement. For series solutions we use enough terms to achieve convergence and numerical results are verified to be independent of mesh discretization.

For operation of the anisotropic membrane, we are interested in the average flux J leaving the core along the line $-R_1 < x < R_1$, y = 0 (Fig. 1b), which is given by

$$\langle J_{I_y} \rangle = -D_I \left\langle \frac{\partial C_I}{\partial y} \right\rangle = -D_I \sum_{n=1}^{\infty} a_n R_1^{n-1}$$
 (9)

Calculation of the fluxes for compounds A and B allow us to predict the selectivity $\alpha_{A/B}$

$$\begin{split} &_{A/B} = \frac{\langle J_{Iy(A)} \rangle / \Delta p_A}{\langle J_{Iy(B)} \rangle / \Delta p_B} \\ &= \left(\frac{D_{I(A)}}{D_{I(B)}} \right) \left(\frac{S_{I(A)}}{S_{I(B)}} \right) \frac{\sum_{n=1}^{\infty} \left[\frac{1 - (-1)^n}{n} \right] \frac{l_A D'_{rA}}{(l_A D'_{rA} + K_A)(R_2 / R_1)^{nl_A} + (l_A D'_{rA} - K_A)(R_2 / R_1)^{-nl_A}}{\sum_{n=1}^{\infty} \left[\frac{1 - (-1)^n}{n} \right] \frac{l_B D'_{rB}}{(l_B D'_{rB} + K_B)(R_2 / R_1)^{nl_B} + (l_B D'_{rB} - K_B)(R_2 / R_1)^{-nl_B}}} \end{split}$$

$$(10)$$

and permeance P_A of the membrane

$$P_{A} = \frac{\langle J_{I_{y}(A)} \rangle}{\Delta p_{A}}$$

$$= \frac{4D_{I(A)}S_{I(A)}}{\pi R_{1}} \sum_{n=1}^{\infty} \left[\frac{1 - (-1)^{n}}{n} \right]$$

$$\frac{l_{A}D'_{rA}}{(l_{A}D'_{rA} + K_{A})(R_{2}/R_{1})^{nl_{A}} + (l_{A}D'_{rA} - K_{A})(R_{2}/R_{1})^{-nl_{A}}}$$
(11)

An analysis of Eq. (10) reveals that the anisotropic separation device introduces a new physical mechanism that can be used to enhance separation. Note that the selectivity can be written as the product of three factors

$$\alpha_{A/B} = \left(\frac{D_{I(A)}}{D_{I(B)}}\right) \left(\frac{S_{I(A)}}{S_{I(B)}}\right) \left(\frac{Q_{(A)}}{Q_{(B)}}\right) \tag{12}$$

where the third factor $Q_{(A)}/Q_{(B)}$ depends on structural and material properties of the anisotropic shell. The ratio $Q_{(A)}/Q_{(B)}$ is equal to one for an isotropic membrane and its existence in our design opens up a number of possibilities in the sense that combinations of structural and material parameters R_1 , R_2 ,l, D'_r ,K can make its value greater than one, thus generating an improvement in the selectivity.

3. Results and discussion

We show in Fig. 2(a) and (b) the selectivity and permeance of the proposed anisotropic membrane in the case of a binary mixture consisting of oxygen and nitrogen. The isotropic core is considered to be polydimethylsiloxane (PDMS) and the homogeneous shell has anisotropic diffusion coefficients D_r and D_{θ} that correspond to a layered structure made of isotropic polymeric materials PDMS and PSF. This will be discussed in detail in the next section. We note that anisotropic membranes are more general and not restricted to layered polymer structures (e.g. they can be made of oriented nanoparticles in a matrix or zeolites). The solubilities and diffusion coefficients for the core and shell materials are summarized in Table 1. The anisotropic shell is purposely designed to detour N_2 around the PDMS core, thus collecting O_2 at the core. This is done by carefully selecting the materials such that the diffusivity ratio $D_{r(\mathrm{O2})}/D_{r(\mathrm{N2})}$ is much larger than the $\mathrm{ratio}D_{\theta(O2)}/D_{\theta(N2)}$. Fig. 2 clearly shows how the structural properties play a fundamental role on the selectivity and permeance. We observe that for a constant value of R_1 the larger the anisotropic shell (i.e. increasing values of R_2/R_1), the higher the selectivity and the lower the

Fig. 2. (a) Selectivity and (b) permeance for our anisotropic membrane device as a function of R_2/R_1 in the case of separation of a binary mixture of oxygen and nitrogen. The cylindrical core is made of PDMS. Red, blue, and green lines correspond to anisotropic, PSF, and PDMS shells respectively. The anisotropic shell is made of layered PSF and PDMS materials. For the permeance, two R_1 values are considered 1 μm and 10 μm.

Table 1 Solubilities and diffusivities for polydimethylsiloxane (PDMS), polysulfone (PSF) [Refs. [42,43]] and for an anisotropic shell made of layered PDMS (M_1) and PSF (M_2) with $f_{PDMS} = 0.5$.

	$S_{(O2)}$ [mol/m 3 Pa]	$D_{(O2)}$ [m ² /s]	$S_{(N2)}$ [mol/m ³ Pa]	$D_{(N2)}$ [m ² /s]	$D_{r (O2)}$ [m ² /s]	$D_{\theta \text{ (O2)}}$ [m ² /s]	$D_{r \text{ (N2)}}$ [m ² /s]	$D_{\theta \text{ (N2)}}$ [m ² /s]
PDMS PSF Shell	7.9×10^{-5} 1.1×10^{-4} 9.45×10^{-5}	3.4×10^{-9} 4.4×10^{-12}	4.0×10^{-5} 6.6×10^{-5} 5.30×10^{-5}	3.4×10^{-9} 1.2×10^{-12}	1.02×10^{-11}	1.42×10^{-9}	2.98×10^{-12}	1.28×10^{-9}

Table 2 Permeabilities for polydimethylsiloxane (PDMS), polysulfone (PSF) and for an anisotropic shell made of layered PDMS (M_1) and PSF (M_2) with $f_{\rm PDMS} = 0.5$.

	P _(O2) [mol/m-Pa-s]	P _(N2) [mol/m-Pa-s]	$P_{r (O2)}$ [mol/m-Pa-s]	$P_{\theta \text{ (O2)}}$ [mol/m-Pa-s]	$P_{r \text{ (N2)}}$ [mol/m-Pa-s]	$P_{\theta \text{ (N2)}}$ [mol/m-Pa-s]
PDMS PSF Shell	2.68×10^{-13} 4.84×10^{-16}	1.36×10^{-13} 7.92×10^{-17}	9.64×10^{-16}	1.34×10^{-13}	1.58×10^{-16}	6.78×10^{-14}

permeance. These results can be understood by considering that by increasing the thickness of the shell, the anisotropic path for the diffusing compounds becomes longer and the effects of the shell on detouring N_2 around the core increase, which increases the selectivity. The increased R_2/R_1 ratio also causes a decrease in the number of molecules that reach the core, thus lowering the permeance. For comparison, we also show the selectivity and permeance in the case that the shell is made of a single isotropic material (either PDMS or PSF). We can see that the separation properties of the proposed device using an anisotropic shell are significantly different from those corresponding to isotropic shells, indicating the possibility of using anisotropic diffusion mechanisms to enhance the separation of O_2 and N_2 Table 2.

A remarkable result from our numerical predictions is that the performance of the proposed anisotropic membranes is above the upper bound limit for most of the permeability spectrum. We show in Fig. 3 the selectivity vs. permeance plot of the device, which is analogous to the well-known Robeson plot [11,12]. A representative value of $R_1 = 1 \, \mu \text{m}$ is chosen for the calculations. The most significant result in Fig. 3 is that the use of an anisotropic shell (red solid line) can make the device to have selectivities significantly higher than the upper bounds (black solid line). For example, for $R_2/R_1 = 2$, the selectivity is two orders of magnitude larger than that from conventional membranes. This demonstrates that control of the direction of the mass flux via anisotropy, as proposed here, can be an important factor in the design

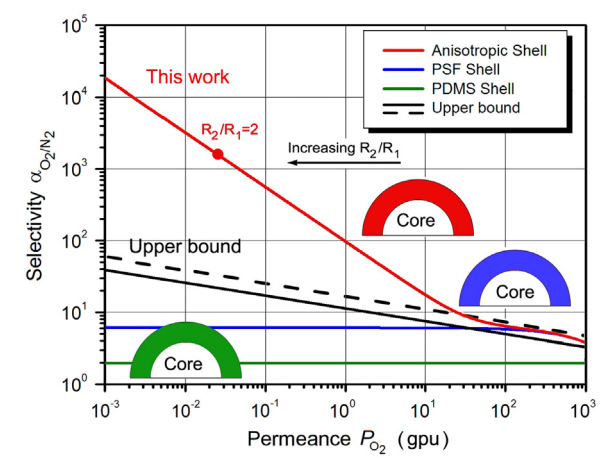


Fig. 3. Modified Robeson plot for selectivity vs. permeance for anisotropic (red), PSF (blue), and PDMS (green) shells respectively where $R_1=1~\mu m$. Black solid and dashed lines shows selectivity vs. permeance upper bounds for a planar isotropic membrane of thickness $1~\mu m$ and $0.1~\mu m$ respectively. We note that if R_1 is increased (reduced) the plot will shift to the left (right).

of separation processes by providing membranes with increased efficiencies. We have also evaluated the collected fraction for increasing R_2/R_1 ratios in the range $1.0 < R_2/R_1 < 3.0$ and found a recovery between ~10% and 0.001%. This indicates that increasing selectivity is accompanied by a reduction in the oxygen recovery. If higher recoveries are needed, larger membrane area and operational costs will be required. For comparison, we also show in Fig. 3 the cases where the shell is made of isotropic materials PDMS (green) and PSF (blue). It should be noted that, in contrast to the anisotropic shell, the selectivity of isotropic shells is bounded by the intrinsic properties of the constituent materials.

As mentioned previously, we propose to manufacture the anisotropic shell using a layered structure made of commonly available isotropic materials. Achieving anisotropic properties by means of bilayer structures has been extensively discussed in the literature [21,26,31,33,34]. According to effective medium theory, it is possible to construct a multilayer structure made of thin layers of alternating materials M_1 and M_2 with different solubilities and diffusivities, which behaves as an anisotropic medium when the number of layers is large enough. The origin of the anisotropicity arises from the fact that, in a layered structure, the resistances to molecular diffusion add in series in one direction and in parallel in the other direction. In our proposed membrane, we have a set of concentric cylinders of alternating materials M_1 and M_2 , in which resistances add in series (parallel) in the radial (azimuthal) direction [Fig. 1(c)]. Effective medium theory establishes the effective radial $D_{r(i)}$ and azimuthal diffusivities $D_{\theta(i)}$ of the layered shell as well as its effective solubility $S_{II(i)}$ in terms of the properties of the isotropic materials and their volume fractions [27,28,35-38], which are given by

$$D_{\theta(i)} = \frac{1}{(f_{M1} + f_{M2}k'_i)} [f_{M1}D_{M1(i)} + f_{M2}k'_iD_{M2(i)}]; [D_{r(i)}]^{-1}$$

$$= (f_{M1} + f_{M2}k'_i) \left[\frac{f_{M1}}{D_{M1(i)}} + \frac{f_{M2}}{k'_iD_{M2(i)}} \right]; S_{II(i)} = f_{M1}S_{M1(i)} + f_{M2}S_{M2(i)}$$
(13)

where $D_{M1(i)}D_{M2(i)}$ are the isotropic diffusion coefficients of compound i in materials M_1 and M_2 respectively, f_{M1} , f_{M2} are the volume fractions, and $k_i' = S_{M2(i)}/S_{M1(i)}$. Using the diffusivities and solubilities given in Table 1 for N_2 and O_2 in PDMS and PSF, Eq. (13) establishes that a multilayer structure made of PDMS (M_1) and PSF (M_2) with $f_{M1}=0.5$ yields the anisotropic properties of the shell previously studied (Table 1). In Fig. 4 we explore the selectivity and permeance as a function of the volume fraction for $R_1=1~\mu m$ and $R_2/R_1=2$. The results show that the volume fraction of the layered shell is another important factor on the performance of the device. The selectivity

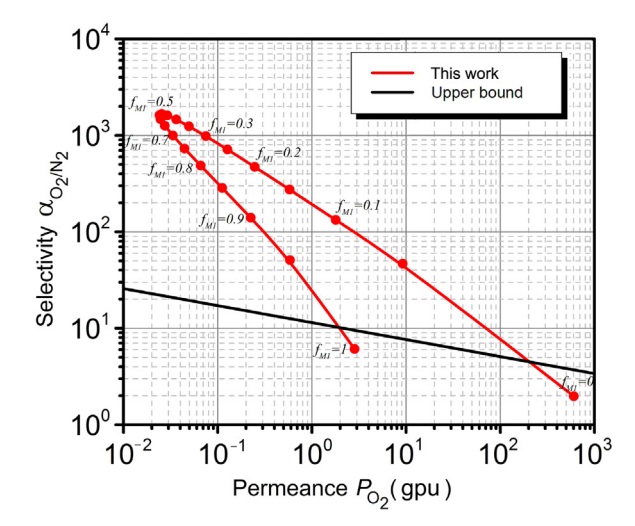


Fig. 4. Selectivity vs. permeance for a membrane separation device with $R_1 = 1 \, \mu \text{m}$ and $R_2/R_1 = 2$ for different volume fractions of PDMS in the shell.

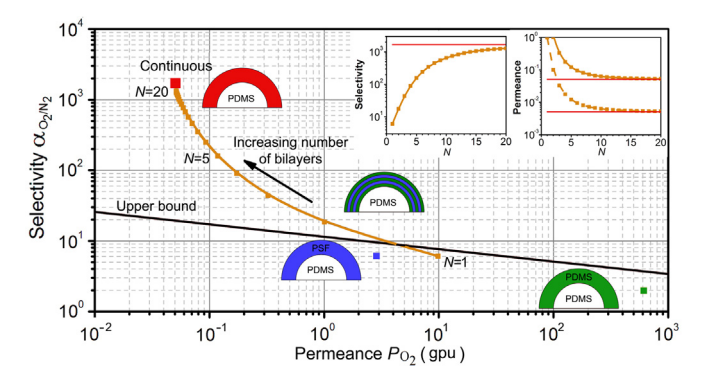


Fig. 5. Insets: Selectivity (left) and permeability (right) of our membrane design for separation of a binary mixture of oxygen (50%) and nitrogen (50%) as a function of the number N of bilayers. The layered anisotropic shell is made of isotropic PDMS and PSF materials. $R_1=1~\mu m$ (top line), $R_1=10~\mu m$ (bottom line) and $R_2/R_1=2$. Main panel: Modified Robeson plot of selectivity vs. permeance for a layered anisotropic shell with $R_1=1~\mu m$ and $R_2/R_1=2$ and increasing number of layers (orange line). For large numbers of bilayers (\sim 20), the performance corresponds to the continuous case (red dot). For reference, PSF and PDMS shells are also shown in the figure. The thickness of each individual layer can be calculated as $(R_2-R_1)/2N$.

increases continuously from $f_{M1}=0$ until it reaches a maximum at $f_{M1}=0.5$ and decreases with further increase of the volume fraction. In contrast, the permeance decreases monotonously until $f_{M1}=0.5$ and increases for larger volume fractions. These results show the richness of behaviors that can be obtained by means of an anisotropic separation device.

We note that another design aspect is the number N of bilayers of materials M_1 and M_2 that are required to obtain an effective anisotropic medium behavior for the shell (Fig. 1c). We thus analyze the role of N in detail in Fig. 5 for an anisotropic shell made of a PDMS-PSF multilayer structure. As it can be seen in the insets, the selectivity increases while the permeance decreases with increasing numbers of bilayers, both showing an asymptotic behavior for a large number of layers. Note that the difference between layered and continuous anisotropic shell is minimal for a sufficiently large number of bilayers ($N\sim20$) [33]. Fig. 5 shows that one important consequence of the resultant selectivity/permeance values obtained for different number of bilayers is that the performance of the device in terms of the modified Robeson plot [12] is also a function of N. As a result, N should be selected ensuring that the performance is above the upper bound. Furthermore it is also possible to tailor the number of layers N to tune the permeance of the device.

That is, the number of layers N can also be a variable to control to a certain extent the relation between selectivity and permeance.

We note that standard dip-coating or spray-coating techniques could be used to fabricate prototype layered devices. Viscosity of polymer solution and drying condition will play a role in ensuring uniform layers [39–41]. Our devices however are robust to moderate deviations in layer thickness since simulations show that \pm 20% variation in layer thicknesses creates only \sim 5% variation in permeance and selectivity. Minimization of void formation and polymer intrusion might also need to be considered during the fabrication process.

4. Conclusions

We showed that engineered anisotropic structures can give rise to a new class of membranes that can improve the performance of separation processes. By controlling the flux direction by means of anisotropy, we introduced a new device for separation that allows increasing the selectivity of membranes above the limits typically observed in isotropic membranes. Interestingly, the anisotropic membranes proposed here can be fabricated as multilayer structures made of two isotropic materials with contrasting diffusivities. The effective diffusivities and solubilities of the anisotropic structure can be obtained using effective medium theory. Importantly, the present work is the first demonstration of a completely new physical system that breaks the separation limits in membrane technologies. Future work would involve the development of manufacturing and miniaturization techniques, as well as strategies for membrane modules in order to fully take advantage of the unprecedented opportunities provided by anisotropic membranes.

Acknowledgments

This work is supported by the National Science Foundation [Grant no. 1744212].

References

- D.F. Sanders, Z.P. Smith, R. Guo, L.M. Robeson, J.E. McGrath, D.R. Paul, B.D. Freeman, Energy-efficient polymeric gas separation membranes for a sustainable future: a review, Polymer 54 (2013) 4729–4761.
- [2] Oak Ridge National Laboratory, Materials for Separation Technologies: Energy and Emission Reduction Opportunities, Oak Ridge, 2005.
- [3] D.S. Sholl, R.P. Lively, Seven chemical separations to change the world, Nature 532 (2016) 435–437.
- [4] P. Bernardo, E. Drioli, G. Golemme, Membrane gas separation: a review/state of the art, Ind. Eng. Chem. Res. 48 (2009) 4638–4663.
- [5] W.J. Koros, C. Zhang, Materials for next-generation molecularly selective synthetic membranes, Nat. Mater. 16 (2017) 289–297.
- [6] M.L. Jue, R.P. Lively, Targeted gas separations through polymer membrane functionalization. React. Funct. Polym. 86 (2015) 40–43.
- [7] R.W. Baker, B.T. Low, Gas separation membrane materials: a perspective, Macromolecules 47 (2014) 6999–7013.
- [8] R.W. Baker, Future directions of membrane gas separation technology, Ind. Eng. Chem. Res. 41 (2002) 1393–1411.
- [9] J.G. Wijmans, R.W. Baker, The solution-diffusion model: a review, J. Membr. Sci. 107 (1995) 1–21.
- [10] P. Pandey, R.S. Chauhan, Membranes for gas separation, Prog. Polym. Sci. 26 (2001) 853–893.
- [11] B.D. Freeman, Basis of permeability/selectivity tradeoff relations in polymeric gas separation membranes, Macromolecules 32 (1999) 375–380.
- [12] L.M. Robeson, The upper bound revisited, J. Membr. Sci. 320 (2008) 390-400.
- [13] M.H. Klopffer, B. Flaconneche, Transport properties of gases in polymers: bibliographic review, Oil Gas Sci. Technol. 56 (2001) 223–244.
- [14] W.J. Koros, G.K. Fleming, Membrane-based gas separation, J. Membr. Sci. 83 (1993) 1–80.
- [15] W.J. Koros, G.K. Fleming, S.M. Jordan, T.H. Kim, H.H. Hoehn, Polymeric membrane materials for solution-diffusion based permeation separations, Prog. Polym. Sci. 13 (1988) 339–401.
- [16] W.J. Koros, M.R. Coleman, D.R.B. Walker, Controlled permeability polymer membranes, Annu. Rev. Mater. Sci. 22 (1992) 47–89.
- [17] K. Li, D. Wang, D. Li, W.K. Teo, Internally staged permeator prepared from annular hollow fibers for gas separation, AIChE J. 44 (1998) 849–858.
- [18] B. Liu, X. Wu, G.G. Lipscomb, J. Jensvold, Novel internally staged permeator designs using a hollow fiber fabric, Sep. Sci. Technol. 35 (2000) 1153–1177.
- [19] M. Sidhoum, S. Majumdar, K.K. Sirkar, An internally staged hollow-fiber permeator for gas separation, AIChE J. 35 (1989) 764–774.

- [20] L. Zeng, R. Song, Controlling chloride ions diffusion in concrete, Sci. Rep. 3 (2013) 3359.
- [21] S. Guenneau, T.M. Puvirajesinghe, Fick's second law transformed: one path to cloaking in mass diffusion, J. R. Soc. Interface 10 (2013) 20130106.
- [22] S. Guenneau, D. Petiteau, M. Zerrad, C. Amra, T. Puvirajesinghe, Transformed Fourier and Fick equations for the control of heat and mass diffusion, AIP Adv. 5 (2015) 053404.
- [23] S. Narayana, Y. Sato, Heat flux manipulation with engineered thermal materials, Phys. Rev. Lett. 108 (2012) 214303.
- [24] E.M. Dede, T. Nomura, P. Schmalenberg, J. Seung Lee, Heat flux cloaking, focusing, and reversal in ultra-thin composites considering conduction-convection effects, Appl. Phys. Lett. 103 (2013) 063501.
- [25] R. Schittny, M. Kadic, S. Guenneau, M. Wegener, Experiments on transformation thermodynamics: molding the flow of heat, Phys. Rev. Lett. 110 (2013) 195901.
- [26] J.M. Restrepo-Flórez, M. Maldovan, Mass separation by metamaterials, Sci. Rep. 6 (2016) 21971.
- [27] J. Sax, J.M. Ottino, Modeling of transport of small molecules in polymer blends: application of effective medium theory, Polym. Eng. Sci. 23 (1983) 165–176.
- [28] N. Shah, J.E. Sax, J.M. Ottino, Influence of morphology on the transport properties of polystyrene/polybutadiene blends: 2. Modelling results, Polymer 26 (1985) 1239–1246.
- [29] J. Csernica, R.F. Baddour, R.E. Cohen, Gas permeability of a polystyrene/poly-butadiene block copolymer possessing a misorientated lamellar morphology, Macromolecules 22 (1989) 1493–1496.
- [30] D.J. Kinning, E.L. Thomas, J.M. Ottino, Effect of morphology on the transport of gases in block copolymers, Macromolecules 20 (1987) 1129–1133.
- [31] J.-M. Restrepo-Flórez, M. Maldovan, Metamaterial membranes, J. Phys. D. Appl. Phys. 50 (2017) 25104.

- [32] F.P. Incropera, D.P. DeWitt, T.L. Bergman, A.S. Lavine, Fundamentals of Heat and Mass Transfer, John Wiley & Sons, Inc, 2007.
- [33] J.M. Restrepo-Flórez, M. Maldovan, Rational design of mass diffusion metamaterial concentrators based on coordinate transformations, J. Appl. Phys. 120 (2016) 084902.
- [34] S. Guenneau, C. Amra, D. Veynante, Transformation thermodynamics: cloaking and concentrating heat flux, Opt. Express 20 (2012) 8207–8218.
- [35] I.V. Belova, G.E. Murch, Analysis of the effective diffusivity in nanocrystalline materials, J. Metastable Nanocrystalline Mater. 19 (2004) 25–34.
- [36] I.V. Belova, G.E. Murch, Diffusion in nanocrystalline materials, J. Phys. Chem. Solids 64 (2003) 873–878.
- [37] C.D. Van Siclen, Effective diffusivity of solute in multiphase materials with segregation, J. Phys. Chem. Solids 65 (2004) 1199–1200.
- [38] Y. Zhang, L. Liu, On diffusion in heterogeneous media, Am. J. Sci. 312 (2012) 1028–1047.
- [39] J. Borges, J.F. Mano, Molecular interactions driving the layer-by-layer assembly of multilayers, Chem. Rev. 114 (2014) 8883–8942.
- [40] J.J. Richardson, M. Björnmalm, F. Caruso, Technology-driven layer-by-layer assembly of nanofilms, Science 348 (2015) (80-.).
- [41] A.R. Ajitha, M.K. Aswathi, M. H.J., J. Izdebska, S. Thomas, Multicomponent Polymeric Materials, Springer, Dordrecht, 2016.
- [42] T.C. Merkel, V.I. Bondar, K. Nagai, B.D. Freeman, I. Pinnau, Gas sorption, diffusion, and permeation in poly(dimethylsiloxane), J. Polym. Sci. Part B Polym. Phys. 38 (2000) 415–434
- [43] J.S. McHattie, W.J. Koros, D.R. Paul, Gas transport properties of polysulfones: 1. Role of symmetry of methyl group placement on bisphenol, Polymer 32 (1991) 840–850.